

Sodium-ion diffusion and ordering in single-crystal  $P2\text{-Na}_x\text{CoO}_2$ G. J. Shu<sup>1</sup> and F. C. Chou<sup>1,2,\*</sup><sup>1</sup>Center for Condensed Matter Sciences, National Taiwan University, Taipei 10617, Taiwan<sup>2</sup>National Synchrotron Radiation Research Center, HsinChu 30076, Taiwan

(Received 7 May 2008; published 8 August 2008)

Sodium-ion self-diffusion in  $P2(\gamma)\text{-Na}_x\text{CoO}_2$  has been studied using a single crystal as an electrode. Mass transport and thermodynamic properties of Na ions were measured by the potentiostatic intermittent titration technique on a single-crystal electrode with greater accuracy under well-defined diffusion geometry. Excluding the significantly slower diffusion behavior near particular Na ordered phases, average diffusion coefficients  $D_{\text{Na}}$  are extracted to be  $1.2 \pm 0.5 \times 10^{-7}$  cm<sup>2</sup>/s for  $x > 0.5$  and  $4.1 \pm 0.5 \times 10^{-8}$  cm<sup>2</sup>/s for  $x < 0.5$ , respectively. The existence of stable phases with special Na ordering of  $x \sim 0.25, 0.33, 0.43, 0.5, 0.55$ , and  $0.71$  are verified by either the maximum or diverging signature of the  $x$ -dependent self-diffusion coefficients.

DOI: 10.1103/PhysRevB.78.052101

PACS number(s): 61.50.Nw, 63.22.Np, 65.40.gk, 66.30.-h

$P2\text{-Na}_x\text{CoO}_2$  (also called  $\gamma$ -structure, space-group  $P6_3/mmc$ ) has a different layered structure to the well-known cathode material  $O3\text{-Li}_x\text{CoO}_2$  (also called  $\alpha$ -structure, space-group  $R\bar{3}m$ ) used in rechargeable lithium batteries. There are two Na layers per unit with prismatic local oxygen environment in the  $P2$  phase and three Li layers per unit cell with octahedral local oxygen environment in the  $O3$  phase sandwiched between triangular lattice Co layers.  $P2\text{-Na}_x\text{CoO}_2$  has regenerated great interest in the field of condensed-matter physics since the discovery of superconductivity ( $T_c \sim 4.2$  K) in  $\text{Na}_{0.33}\text{CoO}_2 \cdot 1.4 \text{H}_2\text{O}$  by Takada *et al.*<sup>1</sup> Rich physical properties from antiferromagnetic magnetic ordering ( $0.75 \leq x \leq 0.85$ ) to metal-to-insulator transitions ( $x=0.5$ ) exist within the phase diagram of  $\text{Na}_x\text{CoO}_2$  as a function of  $x$ .<sup>2,3</sup> Through careful chemical or electrochemical deintercalation procedure, stable phases of particular Na ordering are found at  $x$  near  $0.84, 0.71, 0.5, 0.33$ , and  $0.25$ .<sup>2,4-6</sup> Less well-defined stable phases have also been found at  $x \sim 0.55$  and  $0.43$ .<sup>5</sup> Many energetically favored  $x$  values have been predicted theoretically through density function theory (DFT) calculation;<sup>7</sup> however, not all predicted ordering patterns can be isolated and verified experimentally with success. In particular, the commonly referred Na level of  $x \sim 0.75 = 3/4$  or  $x \sim 0.67 = 2/3$  turns out not to be the most stable phase among  $x > 1/2$ , and  $x=0.71$  shows a clear superstructure formed by Na vacancy ordering of special stability.<sup>4,5</sup> Na ordering and its impact on the Fermi surface has been found to be the key factor that separates the Curie-Weiss metal ( $x > 0.5$ ) and Pauli metal ( $x < 0.5$ ) of distinctly different physical properties, let alone the interesting  $x=0.5$  ordered phase that shows metal-to-insulator transition below  $\sim 51$  K.<sup>8,9</sup> The reconstructed Fermi surface as a result of Na superstructure has been clearly demonstrated by the Shubnikov-de Haas (SdH) oscillation effect by Balicas *et al.*,<sup>10</sup> where the existence of small Fermi-surface pockets originate from the significantly reduced first Brillouin zone due to Na ordering.

Na(Li) ions can diffuse in and out of the host oxygen cage within the layered  $\text{CoO}_2$  two-dimensional (2D) network as the bottleneck formed by the oxygen cage is comparable to the Na(Li) ion size. The diffusion mechanism has been studied extensively in the  $O3\text{-Li}_x\text{CoO}_2$  system for its required

fast Li ion mobility as a rechargeable cathode for the battery. However, the magnitude of the chemical diffusion coefficient,  $\bar{D}_{\text{Li}}$ , has been estimated to be in a wide range from  $10^{-7}$  to  $10^{-13}$  cm<sup>2</sup>/s in the literature, mostly studied through polycrystalline electrode. Significant error could be attributed to the different assumptions of geometry used in the calculation.<sup>11-18</sup> In addition, the major difference of local oxygen environment near Na(Li) ions of  $P2$  and  $O3$  structures is not addressed, where the Na ion sits at  $(2/3, 1/3, 1/4)$  in a  $\text{NaO}_6$  prismatic cage for the  $P2$  structure and the Li ion sits within an octahedral cage for the  $O3$  structure as shown in Fig. 1. Using the single-crystal electrode of well-defined diffusion geometry and the potentiostatic intermittent titration technique (PITT) of small steps (25 mV),<sup>19</sup> we are able to extract highly accurate diffusion coefficient  $D_{\text{Na}}$  in  $P2\text{-Na}_x\text{CoO}_2$  and compare with that of  $O3\text{-Li}_x\text{CoO}_2$  obtained from polycrystalline electrode in the literature. The obtained  $D_{\text{Na}}$  values show clear divergent behavior near  $x \sim 0.71, 0.5, 0.33$ , and,  $0.25$ , which suggests that Na ions prefer to stabilize at these levels and form Na ordered patterns as revealed by the superstructure shown in Laue diffraction patterns.<sup>4,5</sup> In addition, significant reduction of  $D_{\text{Na}}$  is found for  $x \sim 0.55$  and  $0.43$ , which supports the existence of stable phase for-

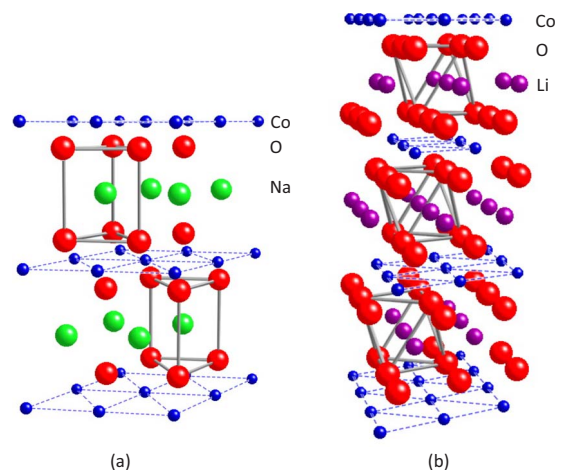


FIG. 1. (Color online) Crystal structures of (a)  $P2(\gamma)\text{-Na}_x\text{CoO}_2$  and (b)  $O3(\alpha)\text{-Li}_x\text{CoO}_2$ .

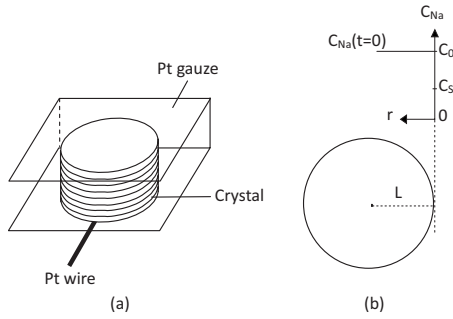


FIG. 2. (a) A schematic of the working electrode used for Na deintercalation, where layered single crystal is sandwiched between Pt gauze of 100 mesh and compressed with a spring-loaded pressure to make sure proper electrical contact. (b) A representative diagram to show a disk shape sample with simplified 1D description of boundary conditions.

mation and its related exotic physical properties.<sup>5</sup>

We used the single crystal grown by the floating-zone technique as an electrode for the diffusion study in this work. A  $\text{Na}_{0.9}\text{CoO}_2$  feed rod has been prepared from a stoichiometric mixture of  $\text{Co}_3\text{O}_4$  and  $\text{Na}_2\text{CO}_3$  powder and a rapid heating procedure is applied at 1023 K for 12 h several times.<sup>21</sup> A high density feed rod of  $10 \text{ cm} \times \varnothing 4\text{--}5 \text{ mm}$  is cold pressed and annealed at 1143 K for 12 h in the air. A single crystal is pulled out from the congruent melt of  $\text{Na}_{0.9}\text{CoO}_2$  feed at a rate of 3 mm/h using a four-mirror optical floating-zone furnace. High gas pressure of 0.75 MPa ( $\text{O}_2:\text{Ar}=4:1$ ) has been applied in the growth chamber in order to improve the growth stability and phase purity.<sup>22</sup> Sodium loss has been prevented with great care and the final Na content is checked by electron probe microanalysis (EPMA) to be near 0.82–0.84 always. The electrochemical cell is set up as  $\text{Na}_{0.84}\text{CoO}_2/1\text{N NaClO}_4$  in propylene carbonate/platinum at room temperature in the air with a Ag/AgCl reference electrode. As shown in Fig. 2(a), single-crystal  $\text{Na}_{0.84}\text{CoO}_2$  is cut into a disk shape of diameter  $\sim 2 \text{ mm}$  with 0.1 mm thickness and sandwiched between spring-loaded platinum gauze. While a constant potential higher than the open-circuit potential (OCP) is applied to the electrode surface, Na ions are deintercalated from the anodic sample electrode until the OCP is equal to the applied voltage  $V_{\text{app}}$ .<sup>5,23</sup> The potentiostatic intermittent titration technique is applied to the sample electrode made of the  $\text{Na}_{0.84}\text{CoO}_2$  single crystal.<sup>19</sup> A series of constant potential  $V_{\text{app}}$  from  $-0.2$  to  $2.2 \text{ V}$  (vs the Ag/AgCl reference electrode) in steps of 25 mV are used in this study. Since the OCP is close to  $-0.25 \text{ V}$  and the induced current is relatively unstable for  $-0.25 < V_{\text{app}} < -0.2 \text{ V}$ , the first reliable data set obtained corresponds to  $x \sim 0.75$ . In each voltage step, the induced current must saturate to a near constant level after 12 h before stepping up to the next  $V_{\text{app}}$ .

In response to a voltage step, the diffusion of Na ions from  $\text{Na}_x\text{CoO}_2$  to the solid-electrolyte interface can be modeled based on Fick's second law within one dimension as

$$\frac{\partial C_{\text{Na}}(r, t)}{\partial t} = \tilde{D}_{\text{Na}} \frac{\partial^2 C_{\text{Na}}(r, t)}{\partial r^2},$$

where boundary conditions of (i)  $C_{\text{Na}} = C_0$  for  $0 \leq r \leq L$ ,  $t = 0$ ; (ii)  $C_{\text{Na}} = C_s$  for  $r = 0$ ,  $t > 0$ ; and (iii)  $\frac{\partial C_{\text{Na}}}{\partial r} = 0$  for  $r = L$ ,

$t \geq 0$  are being used. The geometry of the diffusion discussed is shown in Fig. 2(b).  $\tilde{D}_{\text{Na}}$  represents chemical diffusion coefficient and  $r$  is the distance from the solid-electrolyte interface into the crystal. Based on the exact solution of the above equation,<sup>24</sup>

$$I(t) = \frac{2zFS(C_s - C_0)\tilde{D}_{\text{Na}}}{L} \sum_{n=0}^{\infty} \exp\left(-\frac{(2n+1)^2\pi^2\tilde{D}_{\text{Na}}t}{4L^2}\right) \\ \cong I_0 \exp\left(-\frac{\pi^2\tilde{D}_{\text{Na}}t}{4L^2}\right),$$

where  $F$  is the Faraday constant,  $S$  is the cross-section area between the electrolyte and the cathode,  $L$  is the radius of single-crystal  $\text{Na}_x\text{CoO}_2$ , charge number  $z=1$  for the electroactive species Na, and  $(C_s - C_0)$  is the change of Na concentration at the electrolyte-electrode interface. In the long-time limit that satisfies  $\tilde{D}_{\text{Na}}t/4L^2 > 0.1$ , the exact solution of  $I(t)$  can be represented using the first term only within an error less than 0.1%.  $\tilde{D}_{\text{Na}}$  can be extracted from the first term approximation of  $I(t)$  easily.

Since  $\text{Na}^+$  ion diffusion is always concurrent with the transport of electrons, an applied voltage in the electrochemical deintercalation process would produce additional internal electric field that enhances ion diffusion.  $\tilde{D}_{\text{Na}}$  usually describes interdiffusion (e.g., ionic and electronic species) and its relationship to the self-diffusion coefficient  $D_{\text{Na}}$  (a direct measure of neutral species) is<sup>25</sup>

$$\tilde{D}_{\text{Na}} = D_{\text{Na}} \Theta = D_{\text{Na}} t_e \frac{\partial \ln a_{\text{Na}}}{\partial \ln C_{\text{Na}}},$$

where the thermodynamic factor  $\Theta$  can be described by a function of electronic transference number  $t_e$ , activity  $a_{\text{Na}}$ , and concentration  $C_{\text{Na}}$ .  $t_e$  of  $\text{Na}_x\text{CoO}_2$  is close to 1 because of its metallic behavior at room temperature for the whole range of  $x$ .<sup>2</sup> Thermodynamic factor  $\Theta$  can thus be obtained independently from the PITT titration curve as<sup>26</sup>

$$\Theta = \frac{\partial \ln a_{\text{Na}}}{\partial \ln C_{\text{Na}}} = -\frac{Fx dV}{RT dx},$$

where  $F$  and  $R$  represent Faraday constant and ideal-gas constant, respectively. With the help of independently obtained  $\tilde{D}_{\text{Na}}$  and  $\Theta$ , we are able to derive the self-diffusion coefficient  $D_{\text{Na}}$  as a function of  $x$ . Figure 3 shows a typical induced current as a function of time after  $V_{\text{app}}$  is raised from the equilibrated level  $-0.2 \text{ V}$  to the next voltage step  $-0.175 \text{ V}$ . At the long-time limit,  $\tilde{D}_{\text{Na}}$  can be extracted easily from the slope of  $\ln I(t)$  as shown in the inset of Fig. 3.<sup>17</sup> Note that the long-time approximation criterion  $\tilde{D}_{\text{Na}}t/4L^2 > 0.1$  must be followed in order to use the first term approximation of  $I(t)$  correctly. We chose the linear region of  $\ln I(t)$  right before the measured current falls into the saturated level or instrument resolution limit of the nA range. Our fitted  $\tilde{D}_{\text{Na}}$  values have been verified to satisfy  $\tilde{D}_{\text{Na}}t/4L^2 > 0.17$  always in order to make sure the approximation condition is met self-consistently.<sup>27</sup> The various degrees of electrolyte permeation in the polycrystalline and thin-film electrodes used in most previous studies would have affected the accuracy on

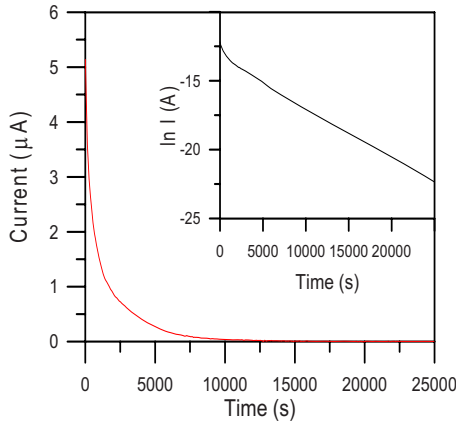


FIG. 3. (Color online) Anodic current versus time in a  $\text{Na}_x\text{CoO}_2$  single-crystal electrode as the applied voltage increases from the equilibrated  $-0.2$  V to a higher step of  $-0.175$  V. The dashed line in the inset is a linear fitting from the long-time limit before induced current is saturated.

the estimation of true dimension, let alone the mixed particle sizes. The single-crystal electrode used in this work has the most accurate dimension in the millimeter range in extracting the value of  $\tilde{D}_{\text{Na}}$ .

The complete results of  $\tilde{D}_{\text{Na}}$  versus  $x$  are shown in Fig. 4(a). We note that there exist four diverging minima near the previously reported Na ordered phases at  $x \sim 0.25$ ,  $0.33$ ,  $0.5$ , and  $0.71$ .<sup>2,3,5</sup> In addition, two local minima exist for  $x \sim 0.43$  and  $0.55$ . Interestingly,  $x \sim 0.43$  is also close to the

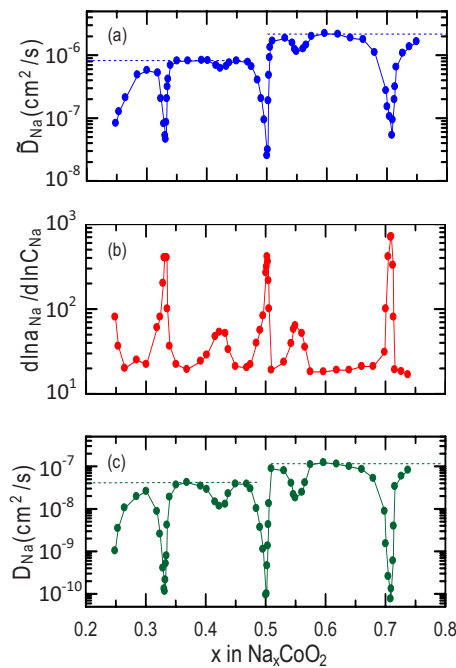


FIG. 4. (Color online) Compositional variation of (a)  $\tilde{D}_{\text{Na}}$ , (b) thermodynamic factor of Na, and (c)  $D_{\text{Na}}$  obtained by the PITT technique at 300 K. The average values of  $D_{\text{Na}}$  excluding the diverging and local minima are  $1.2 \pm 0.5 \times 10^{-7}$   $\text{cm}^2/\text{s}$  for  $x > 0.5$  and  $4.1 \pm 0.5 \times 10^{-8}$   $\text{cm}^2/\text{s}$  for  $x < 0.5$  as indicated by the dashed lines.

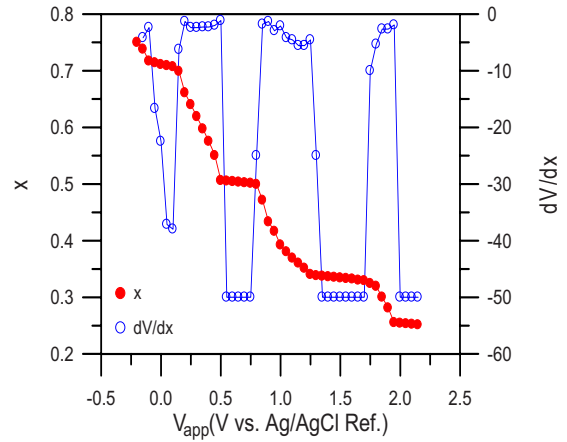


FIG. 5. (Color online) Na concentration  $x$  and  $dV/dx$  versus applied voltage ( $V_{\text{app}}$ ) for  $\text{Na}_x\text{CoO}_2$  starting from  $x=0.75$ .

recently found  $\sqrt{7}a \times \sqrt{7}a$  simple hexagonal surface ordering of surface stoichiometry  $x_s = \frac{3}{7}$ .<sup>28</sup> It is reasonable to connect the behavior of slower diffusion to the particular Na ion ordering of lower free energy. DFT calculation indicates that the primary driving force of Na ordering is screened Coulomb interaction among Na ions.<sup>7</sup> However, the experimentally found Na ordering does not match the predicted patterns from DFT calculation completely,<sup>5</sup> which suggests that other factors such as configuration entropy, electron phonon interaction, and strong electron correlation could also play a role.<sup>4,28</sup> A similar signature of slow-diffusion behavior has been predicted for  $\text{Li}_x\text{CoO}_2$  near  $x=1/3$  and  $1/2$  through calculation,<sup>11</sup> and found experimentally.<sup>27</sup> The first-principles calculations indicate that the activation barriers for Li ion hops into a divacancy site are significantly lower than that of an isolated vacant site in  $O3\text{-Li}_x\text{CoO}_2$ ,<sup>11</sup> where the Li ion hops through the tetrahedral center formed by the oxygens first and then to the vacant site. On the other hand, di-, tri- and quadrivacancy clusters have been proposed and verified through simulation and diffraction techniques for  $P2\text{-Na}_x\text{CoO}_2$  ( $x > 0.5$ ).<sup>4,20</sup> It is interesting to compare the Na ion in  $P2\text{-Na}_x\text{CoO}_2$  of the prismatic oxygen environment and Li ion in  $O3\text{-Li}_x\text{CoO}_2$  of the octahedral environment. For a Na ion to migrate to the nearby monovacancy site, it must pass through the bottleneck formed by the prismatic cage as seen in Fig. 1. However, the nearest-neighbor intermediate vacant site sits directly on top of the Co ion [i.e., Na1 (0,0,1/4) in  $P6_3/mmc$ ], a clearly unfavorable site. On the other hand, such an unfavorable situation is lifted when Na hops to a Na1 site that is closest to the divacancy center, which in turn creates another vacant Na2 site [ $(2/3, 1/3, 1/4)$  in  $P6_3/mmc$ ] and a new form of divacancy is formed by one centered Na1 ion surrounded by three Na2 vacancies, as supported by simulation and Laue diffraction patterns.<sup>4,20</sup>

The thermodynamic factor  $\Theta$  shown in Fig. 4(b) has been extracted independently using  $I(t)$  from the PITT titration curve, where  $dV/dx$  values are derived from the integrated charge in each potential step at room temperature. Similar  $dV/dx$  or  $V$  versus  $x$  plots, as shown in Fig. 5, have been used to demonstrate the occurrence of single phase formation before,<sup>3,23,27</sup> where a single phase sits at the steepest slope of

the  $V$ - $x$  plot. From the occurrence of simultaneous minima/maxima found in  $\tilde{D}_{\text{Na}}$  and  $\Theta$ , it is clear that the diverging peaks or local minima found in  $D_{\text{Na}}$  are related to the Na superstructure formation as demonstrated by the slower diffusivity and lower activity. Excluding the minimum regions of special stability, the average  $D_{\text{Na}}$  values above and below  $x=0.5$  are  $1.2 \pm 0.5 \times 10^{-7}$  and  $4.1 \pm 0.5 \times 10^{-8}$  cm<sup>2</sup>/s, respectively, which are about six orders larger than that obtained from a previous aged single-crystal study.<sup>5</sup> In the previous diffusion study based on an aged single crystal, we fitted a  $C_{\text{Na}}(r, t=2.5 \text{ years})$  spectrum with diffusion equation and solved average  $D_{\text{Na}}$  directly. We believe the large discrepancy comes from the dominant diverging  $D_{\text{Na}}$  near  $x=0.25, 0.33, 0.50,$  and  $0.71$ ; and Na ions in the naturally aged single crystal are trapped in the energetically favored ordered states. The PITT titration technique used in this study provides the extra energy that lifts Na ions from these stable phases of divergent diffusivity.

In summary, using the well-defined diffusion geometry of single-crystal  $\text{Na}_x\text{CoO}_2$  and the PITT technique, we have

been able to determine chemical diffusion coefficient  $\tilde{D}_{\text{Na}}$  and thermodynamic factor  $\Theta$  independently and accurately. The derived Na self-diffusion coefficient,  $D_{\text{Na}}$ , is strongly  $x$  dependent with significant diverging minima for  $x \sim 0.71, 0.50, 0.33,$  and  $0.25$ , in agreement with the existence of special Na ordering at these  $x$  levels. The average values of  $D_{\text{Na}}$  for  $x > 0.5$  and  $x < 0.5$  are accurately determined with the single crystal of well-defined diffusion geometry being  $1.2 \pm 0.5 \times 10^{-7}$  and  $4.1 \pm 0.5 \times 10^{-8}$  cm<sup>2</sup>/s, respectively, which agrees with a picture of dominant faster vacancy diffusion mechanism for a more than half-filled Na layer. Strong suppression of diffusivity due to Na ordering at specific  $x$  in  $\text{Na}_x\text{CoO}_2$  can be a severe obstacle for battery application, but its relatively stable layered structure of wide  $x$  range opens up an important path to understand low dimensional physics *in situ*.

This work was supported by the National Science Council of Taiwan under Project No. NSC-95-2112-M-002.

\*fcchou@ntu.edu.tw

- <sup>1</sup>K. Takada, H. Sakurai, E. Takayama-Muromachi, F. Izumi, D. Dilanian, and T. Sasaki, *Nature (London)* **422**, 53 (2003).
- <sup>2</sup>M. L. Foo, Y. Wang, S. Watauchi, H. W. Zandbergen, T. He, R. J. Cava, and N. P. Ong, *Phys. Rev. Lett.* **92**, 247001 (2004).
- <sup>3</sup>F. C. Chou, J. H. Cho, and Y. S. Lee, *Phys. Rev. B* **70**, 144526 (2004).
- <sup>4</sup>F. C. Chou, M. W. Chu, G. J. Shu, F. T. Huang, W. W. Pai, H. S. Sheu, T. Imai, F. L. Ning, and P. A. Lee, arXiv:0709.0085 (unpublished).
- <sup>5</sup>G. J. Shu, A. Prodi, S. Y. Chu, Y. S. Lee, H. S. Sheu, and F. C. Chou, *Phys. Rev. B* **76**, 184115 (2007).
- <sup>6</sup>L. Viciu, J. W. G. Bos, H. W. Zandbergen, Q. Huang, M. L. Foo, S. Ishiwata, A. P. Ramirez, M. Lee, N. P. Ong, and R. J. Cava, *Phys. Rev. B* **73**, 174104 (2006).
- <sup>7</sup>P. Zhang, R. B. Capaz, M. L. Cohen, and S. G. Louie, *Phys. Rev. B* **71**, 153102 (2005).
- <sup>8</sup>D. Yoshizumi, Y. Muraoka, Y. Okamoto, Y. Kiuchi, J. Yamaura, M. Mochizuki, M. Ogata, and Z. Hiroi, *J. Phys. Soc. Jpn.* **76**, 063705 (2007).
- <sup>9</sup>J. Bobroff, G. Lang, H. Alloul, N. Blanchard, and G. Collin, *Phys. Rev. Lett.* **96**, 107201 (2006).
- <sup>10</sup>L. Balicas, Y. J. Jo, G. J. Shu, F. C. Chou, and P. A. Lee, *Phys. Rev. Lett.* **100**, 126405 (2008).
- <sup>11</sup>A. Van der Ven and G. Ceder, *Electrochem. Solid-State Lett.* **3**, 301 (2000).
- <sup>12</sup>C. H. Chen, E. M. Kelder, and J. Schoonman, *J. Mater. Sci. Lett.* **16**, 1967 (1997).
- <sup>13</sup>C. H. Chen, A. A. J. Buysman, E. M. Kelder, and J. Schoonman, *Solid State Ionics* **80**, 1 (1995).
- <sup>14</sup>J. Barker, R. Pynenburg, R. Koksang, and M. Y. Saidi, *Electrochim. Acta* **41**, 2481 (1996).
- <sup>15</sup>B. Garcia, J. Farcy, J. P. Pereira-Ramos, and N. Baffier, *J. Electrochem. Soc.* **144**, 1179 (1997).
- <sup>16</sup>M. D. Levi, G. Salitra, B. Markovsky, H. Teller, D. Aurbach, U. Heider, and L. Heider, *J. Electrochem. Soc.* **146**, 1279 (1999).
- <sup>17</sup>J. M. McGraw, C. S. Bahn, P. A. Parilla, J. D. Perkins, D. W. Readey, and D. S. Ginley, *Electrochim. Acta* **45**, 187 (1999).
- <sup>18</sup>J. S. Hong and J. R. Selman, *J. Electrochem. Soc.* **147**, 3190 (2000).
- <sup>19</sup>A. H. Thompson, *J. Electrochem. Soc.* **126**, 608 (1979).
- <sup>20</sup>M. Roger, D. J. P. Morris, D. A. Tennant, M. J. Gutmann, J. P. Goff, J.-U. Hoffmann, R. Feyerherm, E. Dudzik, D. Prabhakaran, and A. T. Boothroyd, *Nature (London)* **445**, 631 (2007).
- <sup>21</sup>T. Motohashi, E. Naujalis, R. Ueda, K. Isawa, M. Karppinen, and H. Yamauchi, *Appl. Phys. Lett.* **79**, 1480 (2001).
- <sup>22</sup>D. Prabhakaran, A. Boothroyd, R. Coldea, and N. Charnley, *J. Cryst. Growth* **271**, 74 (2004).
- <sup>23</sup>F. C. Chou, E. T. Abela, J. H. Chob, and Y. S. Lee, *J. Phys. Chem. Solids* **66**, 155 (2005).
- <sup>24</sup>J. Crank, *The Mathematics of Diffusion* (Oxford University Press, London, 1967).
- <sup>25</sup>W. Weppner and R. A. Huggins, *J. Electrochem. Soc.* **124**, 1569 (1977).
- <sup>26</sup>C. J. Wen, B. A. Boukamp, R. A. Huggins, and W. Weppner, *J. Electrochem. Soc.* **126**, 2258 (1979).
- <sup>27</sup>Y.-I. Jang, B. J. Neudecker, and N. J. Dudney, *Electrochem. Solid-State Lett.* **4**, A74 (2001).
- <sup>28</sup>W. W. Pai, S. H. Huang, Y. S. Meng, Y. C. Chao, C. H. Lin, H. L. Liu, and F. C. Chou, *Phys. Rev. Lett.* **100**, 206404 (2008).